Ion exchange and fixation of rare-earth cation into expandable tetrasilicic fluorine mica

Yang-Su Han,[a] Shin-Hei Choi,[a] and Dong-Kuk Kim[a*]

[a]*Department of Chemistry, Kyungpook National University, Taegu 702-701, Korea. Email:kimdk@knu.ac.kr*

Rare-earth cation (Nd^{3+}) are incorporated into the interlayer spaces between the silicate layers of synthetic fluorine mica, $Na_{0.665}Mg_{2.68}(Si_{3.98}Al_{0.02})O_{10.02}F_{1.98}$, by conventional ion exchange reaction. Subsequent migration of the interlayer cations upon calcination into the vacant octahedra of 2:1 layers is followed by powder X-ray diffraction, diffuse-reflectance UV spectroscopy, and X-ray absorption spectroscopy as a function of calcination temperature. It is found from the spectroscopic analyses that the interlayer cations start to migrate into the octahedral vacant sites from 400 °C through the hexagonal siloxane ring of the tetrahedral silicate layers. According to the Nd L_{III}-edge XANES spectra, the normalized absorption intensity gradually decreases while the FWHM increases with temperature, suggesting that the bonding character of rare-earth cations and silicate lattices evolves from ionic to covalent as the calcination temperature increases.

Keywords: layer silicate, ion-exchange, migration, neodymium, XAFS

1. Introduction

Two dimensional layer silicates, in particular, with 2:1 mica-type structures, possess diverse intercalation properties, and therefore have been widely studied for a variety of materials applications including catalysts and catalyst supports, ion exchangers, adsorbents, and ideal inorganic hosts in constructing layer composites with specific functions (Vaccari, 1999). Synthetic Na^+-fluorine mica, which has been synthesized by solid-state intercalation route (Tateyama *et al*., 1992), exhibits good swelling property, high crystallinity and compositional purity, and excellent optical transparency. It is therefore, quite advantageous to employ the synthetic mica as inorganic matrices in designing and architecturing layer nanocomposites with specific photo- and optical properties.

In recent, rare-earth ions doped silica glasses have attracted much interest for optical amplifier and fiber laser applications in telecommunications and high efficient and selective optical band pass color filter in fabricating the flat panel display devices such as plasma display panel (PDP), field emission display (FED), electroluminscent display (ELD), *etc*.(Popeand & Mackenzie, 1988; Fujiyama *et al*., 1990; Strek *et al*., 2000). Typically, alkoxide sol-gel process has been utilized to prepare rare earth-doped silica glasses to achieve the high doping concentrations and the uniform distribution of rare-earth cations (Popeand & Mackenzie, 1988). However, it has been always pointed out that the microscopic clustering of rare-earth ion in silica matrix limits the doping level up to 5 mol% to prevent the concentration quenching.

As an alternative for the conventional alkoxide sol-gel method, the present authors tried a fixation of rare-earth neodymium cation (Nd^{3+}) into layer silicate utilizing the ion exchange property of the synthetic Na-fluorine mica. Ion exchange and fixation of rare-earth cation into anionic charge centers of silicates offers a way of preparing the rare-earth doped silicates with high doping level and homogeneous distribution on an atomic level. In this paper the ion exchange and fixation process of rare-earth cation into layer silicates of mica is investigated by XAFS spectroscopy.

2. Experimentals

2.1 Sample preparation

The starting layer silicate used in this study was a synthetic Na^+-fluorine mica with the chemical formula of $Na_{0.665}Mg_{2.68}(Si_{3.98}Al_{0.02})O_{10.02}F_{1.98}$ (ME-100, CO-OP Chemicals) and the cation exchange capacity (CEC) of 84.5meq./100g. Aqueous Na-mica suspension (2.5 wt%) was prepared and pre-swelled for 1 day prior to the ion exchange reaction. Then the interlayer Na^+ ions of the mica were replaced by neodymium cation (Nd^{3+}) by reacting the mica suspension and aqueous metal solution (0.2 $mol{\cdot}dm^{-3}$) at 60 °C for 48 h. The ion exchange reaction was carried out at a moderate acidic pH (*ca*. 5) to avoid as much as possible the precipitation of metal hydroxides (Bergaya & Damme, 1983). In the ion exchange reaction, the mole ratio of Nd^{3+}/CEC was varied in the range of 0.5 ~ 8.0. The reaction products were separated by centrifugation, washed with deionized water thoroughly, dried under vaccum, and finally heat-treated at the various temperature for 2 h under an ambient atmosphere.

2.2 Sample characterization

Powder X-ray diffraction (XRD) patterns were measured using a X-ray diffractometer (MacScience, MXP-3) equipped with Ni-filtered Cu-Kα radiation (λ=1.5418 Å). Diffuse-reflectance UV-Vis spectra were recorded on a UV-VIS-NIR spectrophotometer, CARY 5G. XAFS spectra were recorded at the beamline 7C at the Photon Factory in the National Laboratory for High Energy Physics (Tsukuba, Japan), operated at 3.0 GeV with *ca*. 400 mA of stored current. A Si (311) crystal was employed in the monochromator. Harmonics were suppressed by detuning 25% from the maximum intensity. The spectra were collected in fluorescence mode using a Lytle detector. Fill-gases used were Ar for the Lytle detector and N_2 for the I_o detector. In the XAS measurement, because of the presence of the Nd L_{II} edges over 6700 eV, only the EXAFS data between 3 ~ $10Å^{-1}$ were extracted and analyzed. These data were k^3-weighted and fourier transformed with a Kaiser window. For EXAFS analysis using UWXAFS code, the bond distance (R), Debye-Waller factor (σ^2), and the coordination number (CN) were optimized as variables in the course of nonlinear least-squares curve fitting between the experimental EXAFS spectrum and the theoretical one that was calculated by *ab-initio* FEFF5 code.

3. Results and discussion

The XRD patterns of Nd-doped mica obtained at different elevated temperatures are represented in Fig.1. The Nd-doped mica heat-treated at 100 °C (a) exhibits a series of reflection lines with a basal spacing of 15.3 Å, indicating that Nd^{3+} ions are stabilized in the gallery space of silicate layers in a double layer hydrated form. Raising the temperature above 200 ~ 300 °C induces a partial dehydration of interlayer water, leading to the transition from double layer to single layer of interlayer water molecules. Surprisingly the single layer hydrated form (d_{001} = 13.3 Å) is stable at least up to ~ 400 °C (b), which can be ascribed to the high polarizing power of rare-earth cations. As the heating temperature increases to 500 °C (c), complete dehydration occurs leading to a d_{001} value of 9.7 Å corresponding to that of the basal spacing of a collapsed clay. The dehydrated lamellar structure remains almost constant up to 800 °C (e), beyond which a complete destruction of the clay structure takes place. The basal spacing (9.7 Å) observed in the dehydrated form

 © 2001 International Union of Crystallography • Printed in Great Britain – all rights reserved

suggests that Nd^{3+} ions migrate into framework region through the hexagonal holes formed by the surface oxygens of tetrahedral silicate layers. It is well known that when metal cations exchanged 2:1-type aluminosilicates are heated, interlayer metal cations migrate into the vacant octahedral sites and neutralize the negativel charge of silicate layers (Sakurai *et al*. 1990). Since diameter of Nd^{3+} (2.22Å) is smaller than that of hexagonal hole (2.52Å), such migration of Nd^{3+} ions into an octahedral vacancy is considered to be feasible. Furthermore, the increase in the intensity of (003) reflection relative to those of (001) and (002) with heating temperature can be explained as follows; as the layer separation decreases, the d_{003} repeat distance approaches the thickness of the individual tetrahedral and octahedral layers in the structure, a value of 3.20 Å. The observed d_{003} value of 3.20 Å also supports the migration and immobilization of Nd^{3+} ions within the framework region (Tennakoon *et al.*, 1986).

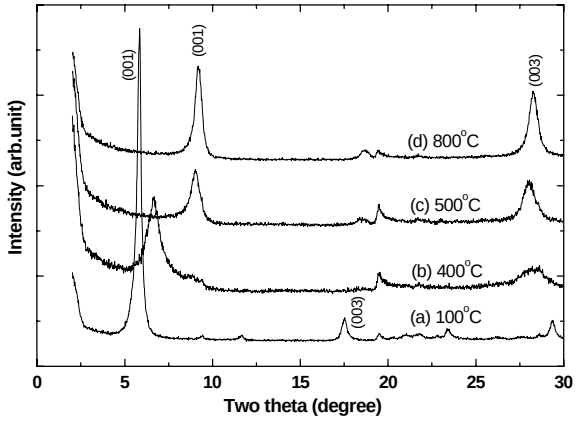

Figure 1
Evolution of powder X-ray diffraction patterns depending upon the heating temperature of the Nd-doped mica.

In order to examine the local environment around Nd^{3+} ions during the migration and fixation into layer silicate lattices, reflection spectra were measured as a function of heating temperature. The typical reflection spectra of the Nd-doped micas are shown in Fig.2 and the assignment of f-f transitions of Nd^{3+} ion is given in the figure according to the literature (Iwamuro *et al*., 1998). In general, the intensities of absorption bands due to the f-f electronic transitions of Nd^{3+} ion decrease with increasing the heating temperature up to 500 ~ 600 °C and then increase again at the higher heating temperature, reflecting the evolution of local environment around the Nd^{3+} ions in the silicate layers; the hydrated-dehydrated-immobilized states as expected from the XRD analysis. It is also interesting to trace the shifts of the 550~640 nm and 794~806 nm peaks, corresponding to the $^4I_{9/2} \rightarrow {}^4G_{7/2}+{}^4G_{9/2}+{}^2K_{13/2}$ and $^4I_{9/2} \rightarrow {}^4F_{5/2}$ transitions (Iwamuro *et al*., 1998), respectively, against the heat treatment temperature. The observed peak positions remain almost constant up to 300 °C, then linearly shifts to longer wavelength when the temperature reaches to 700 °C, beyond which it is more or less established. These spectral shifts reflect that the variation of local environment around Nd^{3+} ions depending upon the heating temperature, that is, Nd^{3+} ions hydrated by interlayer water molecules have a similar chemical environment up to 400 °C. When the interlayer cations start to migrate into octahedral vacant sites through hexagonal siloxane ring above 400 °C, they experience strong negative electric potential exerted by the anionic charge centers of the octahedral layers and a partial charge transfer from anionic sites to metal ions would occur, leading to a partial reduction of Nd^{3+} ions and consequently a spectral red-shift at the higher calcination temperature.

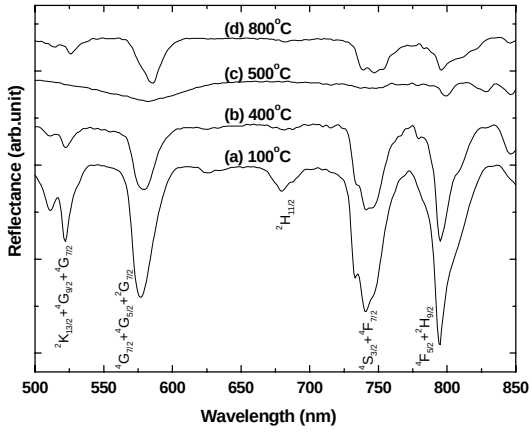

Figure 2
Reflection spectra of the Nd-doped micas as a function of calcination temperature.

The valence state and local environment of the Nd cations were determined from the analysis of the L_{III}-edge XANES spectra of the samples as a function of heating temperature. Fig.3 shows the evolution of Nd L_{III}-edge XANES spectra in the Nd-doped micas. A clear decrease in the intensity and broadening in the full-width at half maxima (FWHM) of the Nd L_{III}-edge resonances (due to $2^2p_{3/2}$-5d electronic transition) is found upon heat-treating the Nd-doped samples. Simultaneously, the absorption maxima slightly shift to the lower energy side as the calcination temperature increases (in the inset of Fig.3). This type of phenonmena can be partially attributed to a decrease of the density of empty d-like states near the Fermi level following Nd migration into the silicate lattices (Hasegawa *et al*., 1998; Tryk *et al*., 1995). As noted before, a surplus negative surface charge of octahedral layers is transfered into cationic Nd ions as they are migrated into vacant octahedral sites upon calcination. The partial donation of negative charge from silicate layers to the $^2D_{5/2}$ and partially filled 4f orbitals of metal cations leads to the lowering the probability of absorption transition and the enhancing the covalent-like character of metal – ligand bonding.

In order to obtain further detailed structural information in the ion-exchange and migration of metal cations into silicate layers, EXAFS analysis was carried out for the Nd-doped mica system. The fourier transform functions and their simulated curves are presented in Fig.4 and the best fitted parameters are listed in Table 1. The FT spectrum of the Nd-mica heat-treated at 100 °C and its simulation (a) yields a single shell of 4 O atoms at a distance of 2.18 Å as nearest neighbors of the central Nd atoms. This indicates that four water molecules are coordinated to Nd^{3+} ions in the form of double layer between the silicate layers, which is well consistent with the XRD result. It should be noted here that the interatomic distance of Nd-O (2.18 Å) is much shorter than that of Nd-O in aqueous solution (2.51 Å) (Yamaguchi *et al*., 1988), which is probably due to the strong electrostatic confinement in the gallery space of silicate layers. As temperature increases to 300 °C (b), the coordination number decreases to 2.4 and the interatomic distance becomes shorter as hydrated water molecules are removed from the interlayer space. Upon dehydration of the interlayer water at around 400 °C, the Nd^{3+} ions begin to migrate into anionic octahedral layers through the hexagonal siloxane hole of tetrahedral silicate layers. Since the diameter of the hexagonal window is 2.52 Å, Nd^{3+} cation with the diameter of 2.22 Å can pass through it into the octahedral cavity. Because the dioctahedral clays like synthetic Na-fluorine mica have vacancies in the octahedral layers, once the cations went through the hexagonal barrier, they occupy quite large free space. The fourier

transform of the experimental spectrum of the sample calcined at 500 °C (c) and its simulation result reveal the presence of three shells. The first peak is best fit with a shell of $1O_1$ at a distance of 2.08 Å. The second one is consistent with a shell of $2O_2$ next-nearest neighbors at a distance of 2.63 Å. Finally, the third is best fit with a shell of 1 Si at an interatomic distance of 3.29 Å. Further increase the temperature to 600 °C (d), the three shells are best fit with $1O_1$-2.06 Å, $1O_2$-2.46 Å, and 1Si-2.70 Å, respectively. This analysis result strongly suggests that the rare-earth cations introduced into hexagonal cavity are situated under highly asymmetric potential spaces. Especially, the metal cations seem to be shifted to negative charge centers, near the octahedral vacancy, to neutralize the excess negative charge. Such evolution of local environments during migration would also influence on the electronic structure of Nd ions, which results in the systematic variation of XANES features.

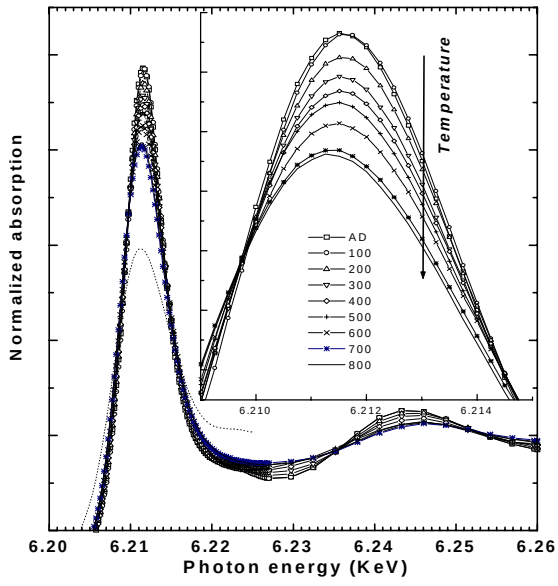

Figure 3
Evolution of Nd L_{III}-edge XANES spectra of the Nd-doped micas as a function of heating temperature.

Table 1
EXAFS derived structural parameters for Nd-doped micas

Temp.(°C)	Shell	C.N	R/Å	$\sigma^2(\times 10^3 Å^2)$
100	Nd-O	4(3.21)	2.18	7.98
300	Nd-O	2(2.14)	2.39	8.73
500	Nd-O_1	1(0.83)	2.08	6.10
	Nd-O_2	2(1.42)	2.63	6.73
	Nd-Si	1(0.83)	3.29	6.63
600	Nd-O_1	1(0.76)	2.06	6.90
	Nd-O_2	1(0.80)	2.46	6.57
	Nd-Si	1(0.80)	2.71	5.10

4. Conclusions

The intercalation of Nd^{3+} ions into the interlayer spaces of silicate layers of synthetic fluorine mica and their subsequent migration into the vacant octahedral sites upon calcination are studied by powder X-ray diffraction, diffuse-reflectance UV spectroscopy, and X-ray absorption spectroscopy as a function of calcination temperature. It is found from the spectroscopic analyses that the interlayer cations start to migrate into the octahedral vacant sites at 400 °C through the hexagonal siloxane ring of the tetrahedral silicate layers. According to the Nd L_{III}-edge XANES and EXAFS analyses, the metal cations are stabilized near the negative charge centers of silicate layers to neutralize the excess negative charge.

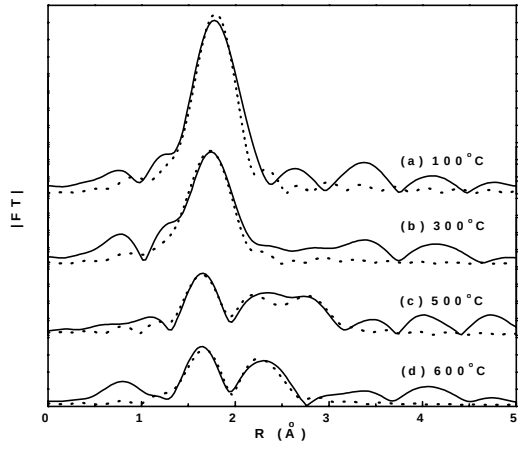

Figure 4
Fourier-transformed radial distribution for the Nd-doped micas. Solid line represents experimental data and dot line corresponds to least-square fits.

This work was supported by the Korea Science and Engineering Foundation (Grant No. 97-05-01-03-01-3), and performed under the proposal (No. 98-G353) of the Photon Factory Program Advisory Committee.

References

Bergaya,F.& Damme,H.(1983). *J.Chem.Soc.-Faraday Trans.*, **79**,505-518.
Fujiyama,T., Hori,M. & Sasaki,M. (1992). *J.Non-Crystal.Solids*, **121**, 273.
Hasegawa,Y., Iwamuro,M., Murakoshi,K., Wada,Y., Arakawa,R., Yamanaka,T., Nakashima,N., & Yanagida,S. (1998). *Bull.Chem.Soc.Jpn.*, **71**, 2573-2581.
Iwamuro, M., Hasegawa, Y., Wada, Y., Murakoshi, K., Nakashima, N., Yamanaka, T. & Yanagida, S. (1998). *J.Luminescence*, **79**, 29-38.
Popeand,E.J.A. & Mackenzie, J.D. (1988). *J.Non-Crystal.Solids*, **106**, 236.
Sakurai,H.,Urabe,K., & Izumi,Y. (1990). *Bull.Chem.Soc.Jpn.*, **63**, 1389-1395.
Strek, W., Pawlik, E., Deren, P., Bednarkiweicz, A., Wokjcik, J., Gaishun, V.E. & Malashkevich, G.I. (2000). *J.Alloys and Compounds*, **300-301**, 459-463.
Tateyama, H., Nishimura, S., Tsunematsu, K., Jinnai,K., Adachi,Y. and Kimura,M. (1992). *Clays and Clay Mineral*, **40**[2], 180-185.
Tennakoon, D.T.B., Thomas, J.M., Jones, W., Carpenter,T.A. and Ramdas,S. (1986). *J.Chem.Soc.-Faraday Trans.*, **82**, 545-562.
Tryk, D.A., Bae, I.T., Scherson, D., Antonio, M.R., Jordan, G.W. and Huston, E.L. (1995). *J.Electrochem.Soc.* **142** [5], L76-L79.
Vaccari,A. (1999). *Appl.Clay Science*, **14**, 161-198.
Yamaguchi, T., Nomura, M., Wakita, H. & Ohtaki, H. (1988). *J.Chem.Phys.*, **89**, 5153

Received 31 July 2000 • Accepted 2 January 2001